

Magnetic properties of spin-1/2 Fermi gases with ferromagnetic interaction

Baobao Wang¹, Jihong Qin^{1, a}, and Huaiming Guo²

¹ Department of Physics, University of Science and Technology Beijing, Beijing 100083, P.R. China

² Department of Physics, Beihang University, Beijing 100191, P.R. China

Received: date / Revised version: date

Abstract. We investigate the magnetic properties of spin-1/2 charged Fermi gases with ferromagnetic coupling via mean-field theory, and find the interplay among the paramagnetism, diamagnetism and ferromagnetism. Paramagnetism and diamagnetism compete with each other. When increasing the ferromagnetic coupling the spontaneous magnetization occurs in a weak magnetic field. The critical ferromagnetic coupling constant of the paramagnetic phase to ferromagnetic phase transition increases linearly with the temperature. Both the paramagnetism and diamagnetism increase when the magnetic field increases. It reveals the magnetization density \bar{M} increases firstly as the temperature increases, and then reaches a maximum. Finally the magnetization density \bar{M} decreases smoothly in the high temperature region. The domed shape of the magnetization density \bar{M} variation is different from the behavior of Bose gas with ferromagnetic coupling. We also find the curve of susceptibility follows the Curie-Weiss law, and for a given temperature the susceptibility is directly proportional to the Landé factor.

PACS. XX.XX.XX No PACS code given

1 Introduction

Magnetism of electron gases has been one of the central issues in condensed matter physics. At low temperature, Fermi particles fill the Fermi level from the lowest energy values, subject to the Pauli exclusion principle, which is different from the Bose gas. Since the observation of Bose-Einstein condensation, the trapped ultracold Fermi gases have attracted great interest [1,2,3,4]. The measurement of magnetic susceptibility for ultracold Fermi gases gives agreement with the Pauli paramagnetism [5]. In the magnetism of magnetized pair-fermion gases, it is shown that the intrinsic spin play an important role in relativistic paramagnetism or diamagnetism [6].

Besides the ideal gases, interaction need to be considered for further understanding the magnetism of quantum gases. While the Heisenberg model can usually be used to explain the magnetic properties of quantum gases. Within the two different large- N formulations, the low-temperature properties of quantum Heisenberg models have been investigated [7], both in ferromagnetic (FM) and antiferromagnetic (AFM) situation. A Heisenberg's FM model has also been used to deal with the high temperature susceptibility [8].

Not only localized electrons, but also the ferromagnetism of itinerant electrons has received a great deal of attention. The development of itinerant electron magnetism

has been outlined with emphasis on spin fluctuations [9]. Research on itinerant ferromagnetism of a trapped two-dimensional atomic gas has shown that the effective interaction strength is unaffected by the particle number density, although the FM phase is enhanced [10]. The FM phase transition of a two-dimensional itinerant electrons Stoner Hamiltonian has been studied with quantum Monte Carlo calculations. It is shown that a first-order FM transition occurred for short screening lengths with a screened Coulomb interaction [11]. In spite of an infinitesimal value of the coupling can induce a FM phase transition for spinor Bose gases [12], the Stoner coupling of Fermi gases cannot lead to a FM phase transition unless it is larger than a threshold. The mechanisms of the Curie-Weiss law for the itinerant electron FM material have been investigated through the $1/d$ expansion theory [13].

In this paper, by using the mean-field theory, the magnetic properties of charged spin-1/2 Fermi gases with FM interactions are investigated. Our results uncover a competition among paramagnetism, diamagnetism and ferromagnetism. We also present a comparison with the results of charged spin-1 Bose gas with FM interactions which have been obtained previously [14]. As the increase of temperature, there is not a pseudo-critical temperature for the charged spin-1/2 Fermi gases with FM interaction, which is different from the case of Bose gas. The relationship of susceptibility and temperature obey the Curie-Weiss law. In section 2, a model consisting of Landau diamagnetism, Pauli paramagnetism and the FM effect is constructed.

^a [jqin@sas.ustb.edu.cn](mailto:jhqin@sas.ustb.edu.cn)

Then the magnetization density and susceptibility are calculated respectively. Section 3 presents a detailed discussion of obtained results. In section 4, we give a brief summary.

2 The Model

We consider a spin-1/2 Fermi gas with FM couplings of N particles, with the effective Hamiltonian written as

$$\bar{H} - \mu N = D_L \sum_{j,k_z,\sigma} (\epsilon_{jk_z}^l + \epsilon_{\sigma}^{ze} + \epsilon_{\sigma}^m - \mu) n_{jk_z\sigma}, \quad (1)$$

where μ is the chemical potential of the system. The quantized Landau levels of the charged fermions are

$$\epsilon_{jk_z}^l = (j + \frac{1}{2})\hbar\omega + \frac{\hbar^2 k_z^2}{2m^*}, \quad (2)$$

where $j = 0, 1, 2, \dots$ labels different Landau levels, and $\omega = qB/(m^*c)$ is the gyromagnetic frequency, with charge q , effective mass m^* and the magnetic induction intensity B . The degeneracy of the Landau levels is

$$D_L = \frac{qBS}{2\pi\hbar c}, \quad (3)$$

where S is the section area of x-y plane of the system.

The Zeeman energy levels associated with the spin degree of freedom,

$$\epsilon_{\sigma}^{ze} = -g\hbar(qB/m^*c)\sigma = -g\sigma\hbar\omega, \quad (4)$$

where g is the Landé factor, and σ denotes the spin-z index of Zeeman state $|F = 1/2, m_F = \sigma\rangle$ ($\sigma = 1/2, -1/2$).

The contribution to the effective Hamiltonian from the FM couplings [15] is

$$\epsilon_{\sigma}^m = -4I\sigma(m + 2\sigma n_{\sigma}), \quad (5)$$

where I denotes FM coupling and spin polarization $m = n_{\frac{1}{2}} - n_{-\frac{1}{2}}$.

Then we obtain the grand thermodynamic potential

$$\begin{aligned} \Omega_{T \neq 0} &= -\frac{1}{\beta} \ln \text{Tre}^{-\beta(\bar{H} - \mu N)} \\ &= -\frac{1}{\beta} D_L \sum_{j,k_z,\sigma} \ln \left[1 + e^{-\beta(\epsilon_{jk_z}^l + \epsilon_{\sigma}^{ze} + \epsilon_{\sigma}^m - \mu)} \right], \end{aligned} \quad (6)$$

where $\beta = 1/(k_B T)$. Through the Taylor expansions and integral over k_z , we have

$$\begin{aligned} \Omega_{T \neq 0} &= -\frac{\omega V}{\hbar^2} \left(\frac{m^*}{2\pi\beta} \right)^{\frac{3}{2}} \sum_{l=1}^{\infty} \\ &\sum_{\sigma} \frac{(-1)^{l+1} l^{-\frac{3}{2}} e^{-l\beta[\frac{1}{2}\hbar\omega - g\sigma\hbar\omega - 4I\sigma(m+2\sigma n_{\sigma}) - \mu]}}{1 - e^{-l\beta\hbar\omega}}, \end{aligned} \quad (7)$$

where V is the volume of the system. A similar treatment has been used to deal with the diamagnetism of scalar

Bose gases [16,17,18]. We have extended it to further study the competition between diamagnetism and paramagnetism of charged spin quantum gases [19,20]. As far as FM interaction is concerned, it is shown that the mean-field theory is still effective in understanding the main physics of magnetism [12,14,15].

Some compact notations for the class of sums are introduced for simplicity,

$$F_{\tau}^{\sigma}[\alpha, \delta] = \sum_{l=1}^{\infty} \frac{(-1)^{l+1} l^{\alpha/2} e^{-l\beta\hbar\omega[\frac{1}{2} - g\sigma - \frac{4I\sigma(m+2\sigma n_{\sigma})}{\hbar\omega} - \frac{\mu}{\hbar\omega} + \delta]}}{(1 - e^{-l\beta\hbar\omega})^{\tau}}. \quad (8)$$

Then we may rewrite equation (7) as

$$\Omega_{T \neq 0} = -\frac{\omega V}{\hbar^2} \left(\frac{m^*}{2\pi\beta} \right)^{\frac{3}{2}} \sum_{\sigma} F_1^{\sigma}[-D, 0], \quad (9)$$

where $D = 3$ is the space dimensionality.

Then the particle number density $n = N/V$ can be obtained through the grand thermodynamic potential,

$$\begin{aligned} n &= -\frac{1}{V} \left(\frac{\partial \Omega_{T \neq 0}}{\partial \mu} \right)_{T,V} \\ &= x \left(\frac{m^*}{2\pi\beta\hbar^2} \right)^{\frac{3}{2}} \sum_{\sigma} F_1^{\sigma}[-1, 0], \end{aligned} \quad (10)$$

where $x = \beta\hbar\omega$.

Taking the grand thermodynamic potential derivative with respect to the magnetic induction intensity B , the total magnetization density can be obtained

$$\begin{aligned} M_{T \neq 0} &= -\frac{1}{V} \left(\frac{\partial \Omega_{T \neq 0}}{\partial B} \right)_{T,V} \\ &= \frac{q\hbar}{m^*c} \left(\frac{m^*}{2\pi\beta\hbar^2} \right)^{\frac{3}{2}} \\ &\sum_{\sigma} \left\{ F_1^{\sigma}[-3, 0] + x \left[\left(g\sigma - \frac{1}{2} \right) F_1^{\sigma}[-1, 0] - F_2^{\sigma}[-1, 1] \right] \right\}. \end{aligned} \quad (11)$$

In external magnetic field H , we have

$$B = H + 4\pi M. \quad (12)$$

It is convenient to introduce some dimensionless parameters, such as $t = T/T^*$, $\bar{M} = m^*cM/(n\hbar q)$, $\bar{\omega} = \hbar\omega/(k_B T^*)$, $\bar{I} = In/(k_B T^*)$, $\bar{\mu} = \mu/(k_B T^*)$, $\bar{m} = m/n$, $\bar{n}_{\sigma} = n_{\sigma}/n$, $\bar{h} = q\hbar H/(m^*c k_B T^*)$, and $x = \bar{\omega}/t$, the characteristic temperature of the system T^* is given by $k_B T^* = 2\pi\hbar^2 n^{\frac{2}{3}}/m^*$. Accordingly, we can re-express equations (10), (11) and (12),

$$1 = \bar{\omega} t^{\frac{1}{2}} \sum_{\sigma} \bar{F}_1^{\sigma}[-1, 0], \quad (13a)$$

$$\bar{M}_{T \neq 0} = t^{\frac{3}{2}}$$

$$\sum_{\sigma} \left\{ \bar{F}_1^{\sigma}[-3, 0] + \frac{\bar{\omega}}{t} \left[\left(g\sigma - \frac{1}{2} \right) \bar{F}_1^{\sigma}[-1, 0] - \bar{F}_2^{\sigma}[-1, 1] \right] \right\}, \quad (13b)$$

$$\bar{\omega} = h + 4\pi\gamma\bar{M}, \quad (13c)$$

where $\gamma = (q^2 n^{1/3}) / (2\pi m^* c^2)$, and

$$\bar{F}_{\tau}^{\sigma}[\alpha, \delta] = \sum_{l=1}^{\infty} \frac{(-1)^{l+1} l^{\alpha/2} e^{-l \frac{\bar{\omega}}{t}} \left[\frac{1}{2} - g\sigma - \frac{4l\sigma(\bar{m} + 2\sigma\bar{n}_{\sigma})}{\bar{\omega}} - \frac{\bar{\mu}}{\bar{\omega}} + \delta \right]}{(1 - e^{-l \frac{\bar{\omega}}{t}})^{\tau}}, \quad (14)$$

where $\bar{\mu}$ is the dimensionless parameter of the chemical potential, which can be determined from the mean-field self-consistent calculations.

At last, we calculated the susceptibility of charged Fermi gases with FM couplings. From the formula $\chi_M = (\frac{\partial M}{\partial H})_{T,V}$, the derivation of equation (11) for the magnetic field H , the expression of susceptibility can be obtained as follows,

$$\chi_M = \frac{\gamma b}{\bar{\omega} - 4\pi\gamma b}, \quad (15)$$

with

$$b = 2\bar{\omega} t^{1/2} \sum_{\sigma} \left\{ \left(g\sigma - \frac{1}{2} \right) \bar{F}_1^{\sigma}[-1, 0] - \bar{F}_2^{\sigma}[-1, 1] \right\} - \bar{\omega}^2 t^{-1/2} \sum_{\sigma} \left\{ 2(g\sigma - 1) \bar{F}_2^{\sigma}[1, 1] - (g\sigma - \frac{1}{2})^2 \bar{F}_1^{\sigma}[1, 0] - 2\bar{F}_3^{\sigma}[1, 2] \right\}. \quad (16)$$

3 Results and discussions

In the following discussions we will focus on the competition of magnetism, and explore the factors that determine the magnetic competition. Meanwhile a comparison with the results of Bose gases with FM coupling will also be presented.

Firstly, the dimensionless magnetization density \bar{M} and $\bar{m} = \bar{n}_{1/2} - \bar{n}_{-1/2}$ versus \bar{I} is shown in figure 1. \bar{I}_c is used to describe the critical value of reduced FM coupling constant of the paramagnetic phase to ferromagnetic phase transition. We can find the crossover of \bar{M} from figure 1(a). When the reduced FM coupling constant \bar{I} is smaller than \bar{I}_c , \bar{M} is always equal to zero. And then \bar{M} begins to increase with increasing \bar{I} from \bar{I}_c . It suggests that there exists a spontaneous magnetization with the increase of \bar{I} in the weak magnetic field. Figure 1(b) indicates that although the value of Landé factor g changes, the evolution of \bar{m} versus \bar{I} almost overlaps. And the value of \bar{I}_c is identical for the given reduced temperature, in despite of the values of Landé factor are different. While the critical value of FM coupling constant \bar{I}_c approximates to 0.5,

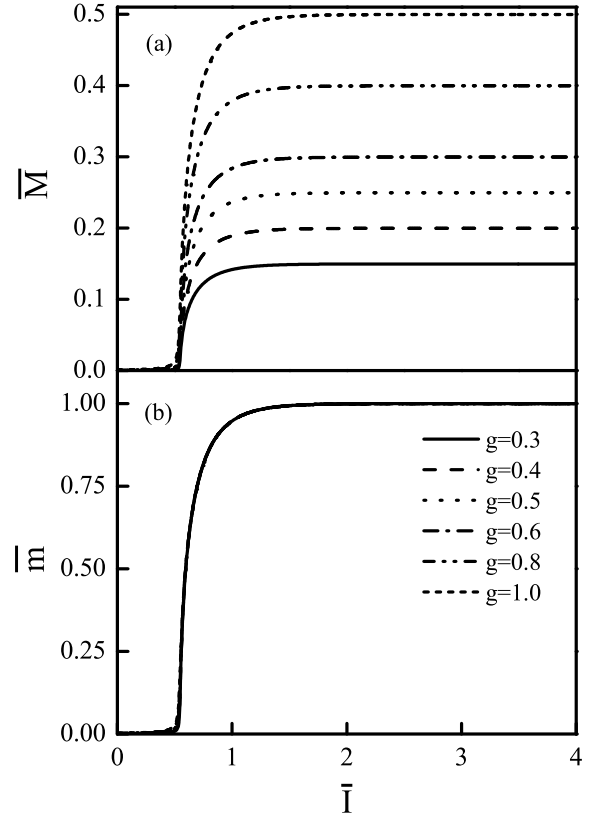


Fig. 1. (a) The reduced magnetization density \bar{M} , (b) $\bar{m} = \bar{n}_{1/2} - \bar{n}_{-1/2}$ as a function of reduced FM coupling constant \bar{I} at reduced temperature $t = 1.5$ and the reduced magnetic field $h = 0.005$. The Landé factor g is chosen as 0.3 (solid line), 0.4 (dashed line), 0.5 (dotted line), 0.6 (dash dotted line), 0.8 (dash dot dotted line), and 1.0 (short dashed line).

which can be evaluated from figure 1. The internal field comes from the spontaneous magnetization results in the diamagnetism [14]. Figure 1 shows that ferromagnetism exceeds the diamagnetism with increasing \bar{I} .

Since \bar{I}_c is an important parameter in the transformation between FM phase and paramagnetic phase. The threshold of \bar{I}_c vs temperature is plotted in figure 2. The FM phase situates above \bar{I}_c , while the paramagnetic phase locates under the \bar{I}_c . We can find that the value of \bar{I}_c increases linearly with the increase of temperature. The results is similar to the Bose gas with FM coupling [14], although they submit to different statistical rules, respectively. It indicates that the crossover from paramagnetic phase to FM phase is more difficult with increasing the temperature.

After studying the spontaneous magnetization in the weak magnetic field, figure 3 is plotted in order to understand the influence of Landé factor g . In figure 3, the magnetic field is chosen as $h = 0.8$ and the reduced temperature $t = 1.5$. The horizontal line $\bar{M} = 0$ in figure 3(a) is used to distinguish the region of paramagnetism and diamagnetism. It is shown that \bar{M} is a negative value

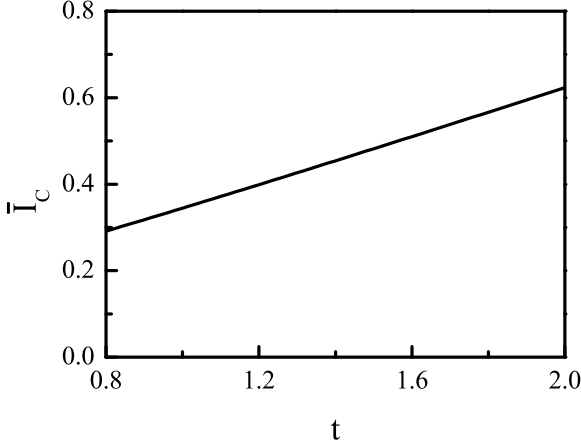


Fig. 2. \bar{I}_c versus reduced temperature t phase diagram of charged spin-1/2 Fermi gases at magnetic field $h = 0.005$.

when g is small, which mainly derives from the diamagnetic contribution. From figure 3(b) we can find that \bar{m} increase with increasing of Landé factor g until approximates saturation at higher \bar{I} . It indicates that the larger \bar{I} the larger \bar{m} for the identical value of Landé factor g , where the Landé factor denotes the intensity of the paramagnetism [19,20]. From figure 3(a) and 3(b), we can find that the enhance of ferromagnetism stimulates the increasing of paramagnetism. That is ferromagnetism cooperates with paramagnetism to confront diamagnetism in a finite magnetic field. This is different from the result of the Bose gas with FM coupling [14]. Where it is faintly affected by the FM coupling in the evolvement of magnetization density with g .

Figure 4 is plotted to get more insight of the dependence of the magnetization density on magnetic field. The system presents diamagnetism when g is small. Furthermore, there exists a threshold g_c when $0.3 < g < 0.6$, which making $\bar{M} < 0$ while $g < g_c$. This is independent of the magnetic field. From the inset of figure 4(a), we can find that the magnetization density approximates to a small positive value at first when $g = 0.6$. While $g \geq 0.6$, the magnetization density increases firstly with increasing the magnetic field, and then declines up to reach a saturation value. It is shown that the paramagnetism competes with diamagnetism in this definite FM coupling situation.

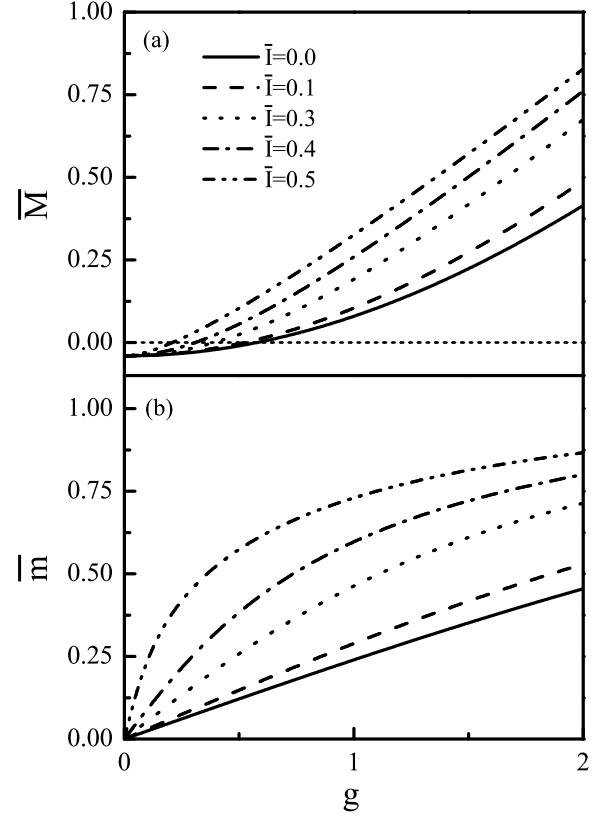


Fig. 3. (a) The reduced magnetization density \bar{M} , (b) $\bar{m} = \bar{n}_{1/2} - \bar{n}_{-1/2}$ versus Landé factor g at reduced temperature $t = 1.5$ and $h = 0.8$, where $\bar{I} = 0.0$ (solid line), 0.1 (dashed line), 0.3 (dotted line), 0.4 (dash dotted line), and 0.5 (dash dot dotted line).

The increasing of Landé factor promotes paramagnetism, while the magnetic field facilitates diamagnetism.

For a more detailed understanding of the paramagnetism and diamagnetism respectively, now we turn to examine the paramagnetization density $\bar{M}_p = g\bar{m}$ and diamagnetization density $\bar{M}_d = \bar{M} - \bar{M}_p$ in figure 5. It is shown that both the paramagnetization density and diamagnetization density increases with enhancing the magnetic field at first. And then the paramagnetization density \bar{M}_p tends to saturate when the magnetic field intensity is strong. While the absolute value of diamagnetization density $|\bar{M}_d|$ increases with the increase of magnetic field intensity. When the magnetic field continues to increase, the diamagnetism is close to a saturated value. Therefore for the higher magnetic field the total magnetization density \bar{M} reaches to saturated values. This is in conformity with the result of figure 4 in qualitatively. With the increase of magnetic field, the contribution come from ferromagnetism, paramagnetism and diamagnetism reach to maximum, so the peak of total magnetization density appears when Landé factor g is 0.8 and 1.0 in figure 4. Whereas the diamagnetism increases faster than paramagnetism as the magnetic field continues to increase.

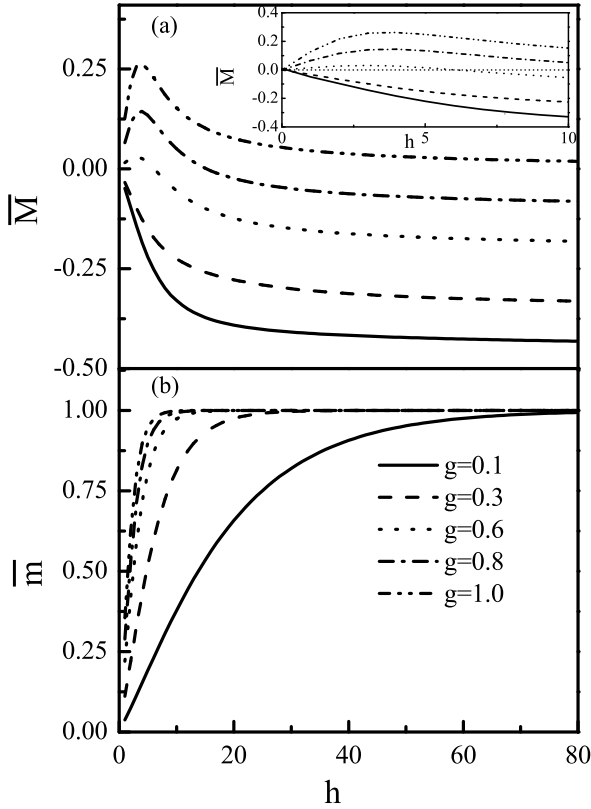


Fig. 4. (a) The reduced magnetization density \bar{M} , (b) $\bar{m} = \bar{n}_{1/2} - \bar{n}_{-1/2}$ as a function of reduced magnetic field h at $t = 1.5$ and $\bar{I} = 0.1$, where Landé factor $g=0.1$ (solid line), 0.3 (dashed line), 0.6 (dotted line), 0.8 (dash dotted line), and 1.0 (dash dot dotted line). The inset of figure 4(a) depicts the relationship of reduced magnetization density \bar{M} versus magnetic field h with the magnetic field region lies between 0 and 10.

It accounts for the total magnetization density decreases with the increase of magnetic field until nearly saturated, which can be found in figure 4.

The characteristic parameter γ has been set to 10^{-6} in figures 1~5, where the particle number density is $8/nm^3$ and the charge and mass are evaluated from a thin electron gas. To further investigate the FM phase transition of the charged spin-1/2 Fermi gases in a broad temperature region including low temperature, $\gamma = 10$ is assumed. Figure 6 shows \bar{M} and \bar{m} as a function of the temperature t when $g = 0.8$ in magnetic field $h = 0.005$. It denotes that the maximal \bar{M} occurs at a definite temperature, and then decreases in both lower temperature and higher temperature regimes. Moreover, \bar{M} decreases faster in the low temperature region than the case of the Bose gas with FM coupling [14]. It reflects the diamagnetism strengthens greatly in this region for Fermi gas. With increasing the temperature, a flat decline appears when \bar{M} is close to zero, which can be seen clearly from the inset of figure 6(a). This is obviously different from the Bose gas. In our previous study on Bose gas with FM coupling

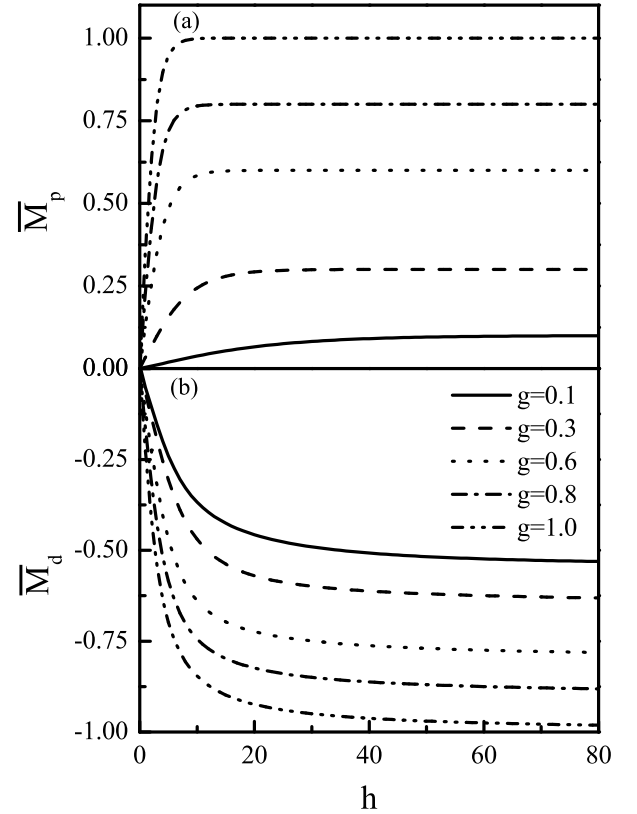


Fig. 5. (a) The reduced paramagnetization density \bar{M}_p , (b) the reduced diamagnetization density \bar{M}_d as a function of reduced magnetic field h at $t = 1.5$ and $\bar{I} = 0.1$, where Landé factor $g=0.1$ (solid line), 0.3 (dashed line), 0.6 (dotted line), 0.8 (dash dotted line), and 1.0 (dash dot dotted line).

[14], a sharp decline emerges when \bar{M} approaches to zero, which suggests that there exists a pseudo-condensate temperature in the transition from ferromagnetism to paramagnetism. However, at high temperature region for the charged Fermi gases with FM interaction, \bar{M} and \bar{m} are asymptotic with respect to the zero point for different values of \bar{I} . This demonstrates that there does not exist the pseudo-critical temperature for Fermi gases. The difference between Fermi gases and Bose gases may be attributed to the different statistical distribution.

Figure 7 plots the evolution of reciprocal of susceptibility with the reduced temperature t , where the characteristic parameter γ is reset as 10^{-6} . It is shown that the curves of $1/\chi$ is proportional to the reduced temperature t . This suggests that the susceptibility of Fermi gases with FM coupling conforms to the Curie-Weiss law. When the temperature is fixed, the susceptibility increases with the increase of the Landé factor g . Since the Landé factor g denotes the strength of paramagnetism, it suggests that the increase of susceptibility is mainly attributed to the contribution of paramagnetism at the fixed temperature and magnetic field.

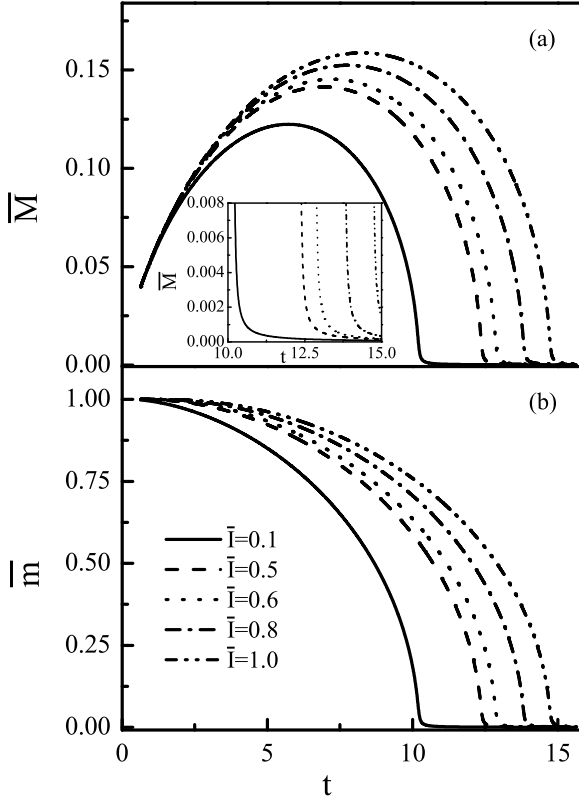


Fig. 6. (a) The reduced magnetization density \bar{M} , (b) $\bar{m} = \bar{n}_{1/2} - \bar{n}_{-1/2}$ versus reduced temperature t at reduced magnetic field $h = 0.005$ and Landé factor $g = 0.8$, where $\bar{I}=0.1$ (solid line), 0.5 (dashed line), 0.6 (dotted line), 0.8 (dash dotted line), and 1.0 (dash dot dotted line). The inset of figure 6(a) depicts the smooth decline of reduced magnetization density \bar{M} with the reduced temperature lies between 10 and 15.

4 Summary

This paper has revealed the interplay among paramagnetism, diamagnetism and ferromagnetism of the charged spin-1/2 Fermi gases with FM interaction. The paramagnetic effect is described by the Landé factor g . Our results show that the ferromagnetism overcomes the diamagnetism when $\bar{I} > \bar{I}_c$ in weak magnetic field. \bar{I}_c increases linearly with the increase of temperature. With increasing g , the gas presents paramagnetism from diamagnetism. The reduced magnetization density \bar{M} declines in the high magnetic field region, which indicates that the contribution comes from diamagnetism enhances in the region of strong magnetic field. As the increase of temperature, the magnetization density asymptotically approximates to zero, which is different from the case of Bose gas with FM coupling. It indicates that there is not a pseudo-critical temperature for charged Fermi gases with FM interaction. The diagram of susceptibility is in accordance with the Curie-Weiss law.

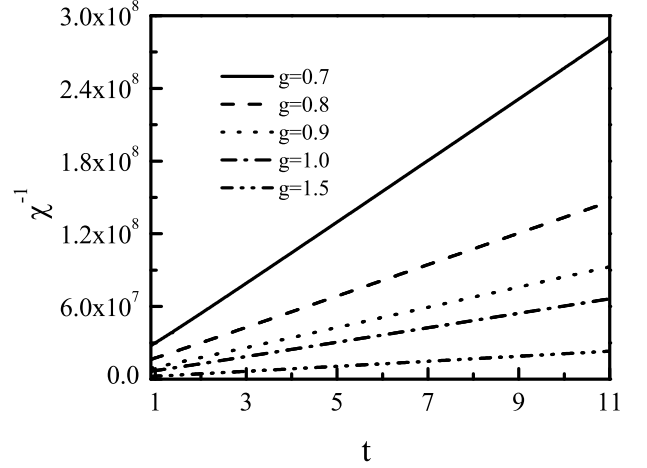


Fig. 7. The reciprocal of susceptibility $1/\chi$ versus reduced temperature t at reduced magnetic field $h = 0.005$ and reduced FM coupling constant $\bar{I}=0.5$. The Landé factors: $g=0.7$ (solid line), 0.8 (dashed line), 0.9 (dotted line), 1.0 (dash dotted line), and 1.5 (dash dot dotted line).

We would like to thank Professor Qiang Gu for the helpful discussions. BW and JQ are supported by the Fundamental Research Funds for the Central Universities under Grant No. FRF-TP-14-074A2, the Beijing Higher Education Young Elite Teacher Project under Grant No. 0389, and the National Natural Science Foundation of China under Grant No. 11004006, and HG is supported by the National Natural Science Foundation of China under Grant No. 11274032.

All authors contributed equally to this paper.

References

1. J. Noronha, D.J. Toms, Phys. Lett. A **267**, 276 (2000)
2. S. Giorgini, L.P. Pitaevskii, S. Stringari, Rev. Mod. Phys. **80**, 1215 (2008)
3. I. Bloch, Nature Physics **1**, 23 (2005)
4. D. Greif, T. Uehlinger, G. Jotzu, L. Tarruell, T. Esslinger, Science **340**, 1307 (2013)
5. Y.R. Lee, T.T. Wang, T.M. Rvachov, J.H. Choi, W. Ketterle, M.S. Heo, Phys. Rev. A **87**, 043629 (2013)
6. J. Daicic, N.E. Frankel, R.M. Gailis, V. Kowalenko, Phys. Rep. **237**, 63 (1994)
7. D.P. Arovas, A. Auerbach, Phys. Rev. B **38**, 316 (1988)

8. G.S. Rushbrooke, P.J. Wood, Proceedings of the Physical Society. Section A **68**, 1161 (1955)
9. T. Moriya, Journal of magnetism and magnetic materials **100**, 261 (1991)
10. G.J. Conduit, Phys. Rev. A **82**, 043604 (2010)
11. G.J. Conduit, Phys. Rev. B **87**, 184414 (2013)
12. Q. Gu, R. A. Klemm, Phys. Rev. A **68**, 031604 (2003)
13. E. Miyai, F.J. Ohkawa, Phys. Rev. B **61**, 1357 (2000)
14. J.H. Qin, X.L. Jian, Q. Gu, J. Phys.: Condensed Matter **24**, 366007 (2012)
15. C.J. Tao, P.L. Wang, J.H. Qin, Q. Gu, Phys. Rev. B **78**, 134403 (2008)
16. D. J. Toms, Phys. Rev. B **50**, 3120 (1994)
17. D. J. Toms, Phys. Rev. D **51**, 1886 (1995)
18. G. B. Standen, D.J. Toms, Phys. Rev. E **60**, 5275 (1999)
19. X.L. Jian, J.H. Qin, Q. Gu, Phys. Lett. A **374**, 2580 (2010)
20. X.L. Jian, J.H. Qin, Q. Gu, J. Phys.: Condensed Matter **23**, 026003 (2011)